

Isolated Multiport converter for Standalone Renewable Energy System

Sharma S
department of EEE
Puducherry Technological University
Puducherry, India
sharma.sha@pec.edu

Rajambal K
department of EEE
Puducherry Technological University
Puducherry, India
rajambalk@pec.edu

Abstract— Multiport converters are being used to integrate renewable energy sources with energy storage, which is attracting a lot of interest. There has been a lot of study on multiport converters. The combination of super capacitors and battery-based hybrid energy storage (HES) is just a very small portion of them. Therefore, a multisource converter structure is suggested in this project with an emphasis on combining super capacitor, battery, wind, and solar. A grid-connected system and supervisory control are created based on the suggested setup. The Super capacitors have built-in voltage regulation, therefore additional voltage sensors and controllers are not necessary. Transient/high-frequency components are naturally sent to the super capacitor, where additional control circuitry and current sensors are not needed to facilitate power-sharing between the battery and the super capacitor. A photovoltaic hybrid converter's duty cycle is nearly constant regardless of load. A transformer is used, enabling galvanic isolation and great voltage gain. The aspects of mathematical modelling, analysis, and design are addressed in depth. Experimental data and computer simulations are used to validate the suggested system. Due to their natural complimentary behavior, photovoltaic (PV) and wind energy hybridization is becoming more and more prevalent. The hybridization of PV and wind worsens power fluctuations, which has a negative impact on the size and lifespan of energy storage. It is possible to significantly minimize the current stress and battery size by using a hybridized energy storage system (a battery and super capacitor combined). Hybrid energy storage (HES) can also manage the system dynamics well. This project intends to integrate many power sources into the grid, including batteries, super capacitors, wind turbines, and photovoltaics (PV). MATLAB/Simulink would be used to create the system's simulation model. The effectiveness would be examined under various operating circumstances, and the findings would be shared.

Keywords—DC to DC converter, Hybrid Energy Storage, Solar PV system, Super Capacitor and Wind Energy System

I. INTRODUCTION

One of the most significant renewable energy sources that has seen growing attention in recent years is solar energy. When compared to other energy sources, solar energy is the most readily available and it is abundant in nature [1]. The sun provides the world with enough energy in a single day to meet all of its energy demands for an entire year. Since solar energy doesn't generate any pollutants or by-products that are damaging to the environment, it is clean and emission-free. Numerous areas can benefit from the conversion of solar energy into electrical energy. Solar thermal and sun photovoltaic systems may both convert solar energy into electrical energy.

Solar photovoltaic systems employ silicon or specific semiconductor-based cells to turn light energy from incoming sunlight into direct current (DC) power [2]. Storage of the produced power into batteries is required to account for intermittent and night time use. Low-cost flat-panel solar panels, thin-film technology, concentrator systems, and many more cutting-edge ideas have all seen a rise in research and development recently [3]. The pricing of small solar power modular units and solar power plants will soon be within the reach of large-scale solar energy production and utilization.

There are known dedicated converter setups for combining diverse sources. The design, analysis and creation of efficient control structures and power/energy management plans is the primary focus of the works that are covered in these article [4]. Having a separate converter for each source, however, makes the control structure more complex and results in lower utilization, greater costs, and worse efficiencies [5]. In order to integrate different sources, multi-input converter configurations that potentially handle the aforementioned problems are attracting a lot of interest [6]. Figure 1 depicts the block diagram of a typical multi-source converter that connects a PV, wind, battery, super capacitor and utility grid.

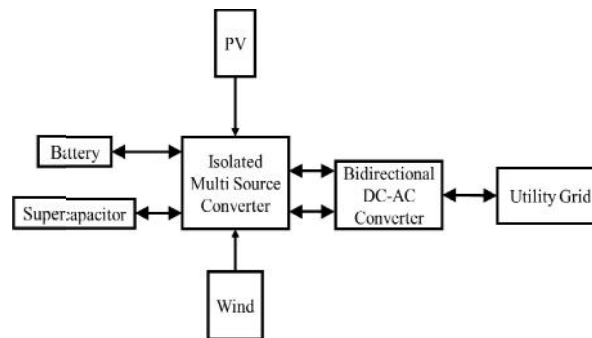


Fig. 1. Block diagram of typical multi-source converter

The multi-port converters have been the subject of significant study that has been published in the literature. The authors suggested a setup for an isolated multiple-input converter that can link two renewable energy sources with energy storage [7]. The configuration provided may interface PV, wind, and energy storage at the same time while having a lower component count than the multi-port converter configurations previously reported [8]. Authors demonstrated multi-port converter setups that could interface with HES and renewable energy sources [9]. To connect hybrid energy storage, the authors in presented a multi-port converter based on a dual active bridge architecture. An additional adjustable port in the topology is used for voltage matching. The additional controller makes it possible to link many storage components at once and significantly lowers reactive power and circulating currents [10]. This design, however, is unsuitable for connecting low-voltage storage components to a high-voltage DC-bus. Authors in [11] offered a high multi-port DC-DC converter as a solution, a modified variant of There are provided multi-port converters based on triple active bridge architecture. In [12] contrast to the full-bridge transformer-coupled topology in, the topologies in are half-bridge transformer topologies. In order to create a multi-port configuration and incorporate a hybrid energy storage system, the transformer-coupled full-bridge converter uses the notion of multiplexing use [13]. A better DC bus voltage controller is also shown [13]. In [14], a consensus-based control method and a cascaded multi-port converter are proposed. The component rating of the second stage converter is significantly reduced by the suggested converter. At the second level of the cascaded structure, this architecture makes it easier to add several batteries [15]. The suggested arrangement has fewer components and is straightforward in this paper.

II. TRANSFORMER-COUPLED HALF-BRIDGE DC-DC BOOST CONVERTER

The DC-DC Boost converter configuration is shown in Fig. 2. In the proposed configuration a transformer-coupled half-bridge DC-DC boost converter is used to interface wind source. On both sides of the high frequency transformer two DC-links are formed [16]. The DC-links on low voltage and high voltage sides are named as primary and secondary DC-links. A series connected PV and hybrid energy storage via bidirectional DC-DC buck-boost converter is connected across the primary DC-link. The battery in series with decoupling inductor is connected across supercapacitor to form an Energy Storage Unit (ESU) with power sharing capability. At the secondary of the DC-link, a GSC (Grid Side Converter) is connected. V_{sc} , V_b , V_s , V_{pv} , V_w , V_{dc1} , V_{dc2} and V_g are the voltages of supercapacitor, battery, ESU, PV, primary DC-link, secondary DC-link and grid respectively. I_{sc} , I_b , I_s , I_{pv} , I_w , I_L and I_g are the currents of super capacitor, battery, ESU, PV, wind, load and grid respectively. C_{sc} and R_{sc} are capacitance and internal resistance of the super capacitor. L_b and R_b are the decoupling inductance and internal resistance of the battery. L_w , L_g and L_{ph} are the inductance of wind converter, GSC and Photovoltaic Hybrid Converter (PHC) respectively. C_{pv} , $C_1 + C_2$ and $C_3 + C_4$ are the capacitance of PV, primary DC-link and secondary DC-link respectively. i_{ph} and v_{ph} are current through and voltage across L_{ph} .

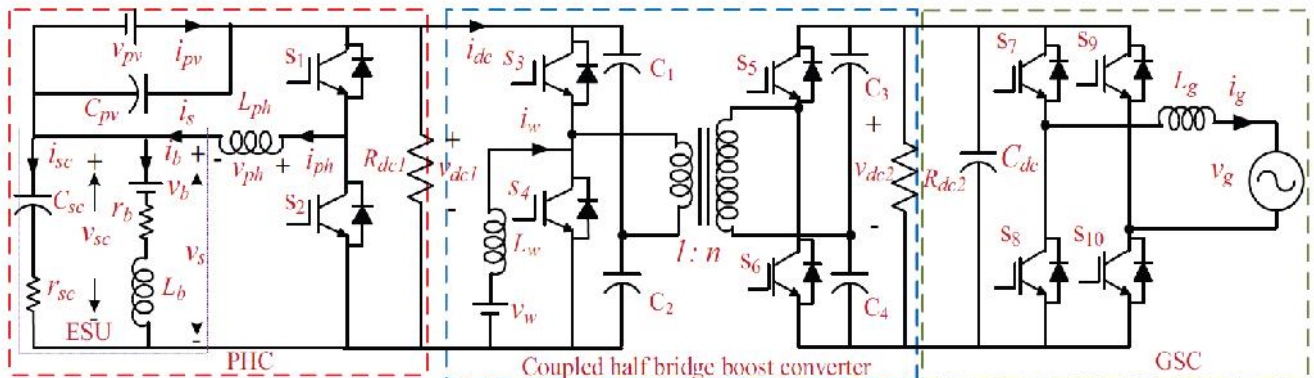


Fig. 2. Isolated grid-connected multi-source converter configuration.

A. Switching equivalent circuit

When PV is available, the current i_{ph} is controlled by operating the switches S1, S2 such that voltage across C_{pv} is at $v_{pv} = v_{mpp}$ which ensures PV operating at MPP (Maximum Power Point). When PV is OFF, voltage across C_{pv} is regulated at $v_{pv} = (v_{dc1r} - v_b)$ by controlling the current i_{ph} . The wind source along with rectifier is considered as a DC-source and the current drawn is controlled by operating the switches S3, S4, S5, S6 such that the current i_w is regulated at i_{wmp} which ensures MPP operation of wind. By controlling the switches S7, S8, S9, S10, grid current i_g is regulated at i_{g} , which is the current required to maintain power balance in the system. The switching equivalent circuits of PHC are shown in Fig. 3 (a), (b). Fig. 3 (c), (d) shows the primary referred switching equivalent circuits of the transformer-coupled half-bridge converter.

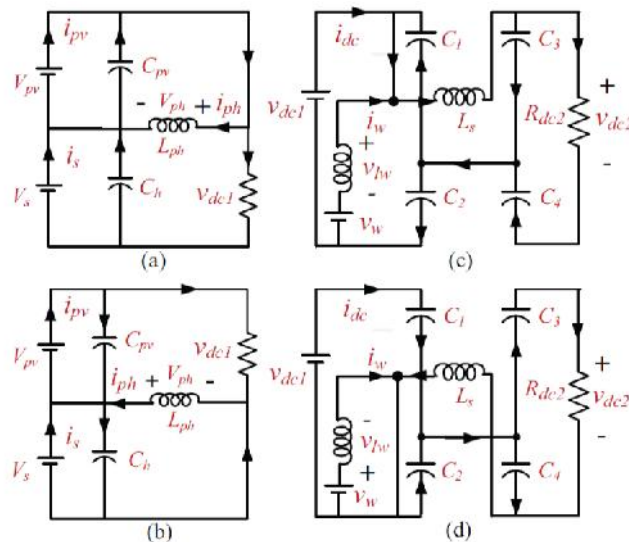


Fig. 3. (a),(b) Switching equivalent circuits of PHC and (c),(d) Switching equivalent circuits of transformer coupled half-bridge converter.

III. CONTROL STRUCTURE FOR THE PROPOSED CONFIGURATION

The control structure is framed such that the power balance in the system is maintained. A hysteresis current controller generates the switching pulses for the grid-connected full-bridge converter. The reference grid current i_{gr} is selected based on the Reference Selection Scheme (RSS). The reference selection scheme is framed based on the SoC of battery, source, and load powers. The reference grid current is selected to be zero when (i) Source Power generated is greater than the load power, and SoC is less than SoCmax. (ii) Source power generated by PV and wind is less than the load Power, SoC is greater than SoCmin. The reference grid current is selected to be i_{req} for all the remaining cases. A Proportional Integral (PI) controller generates the



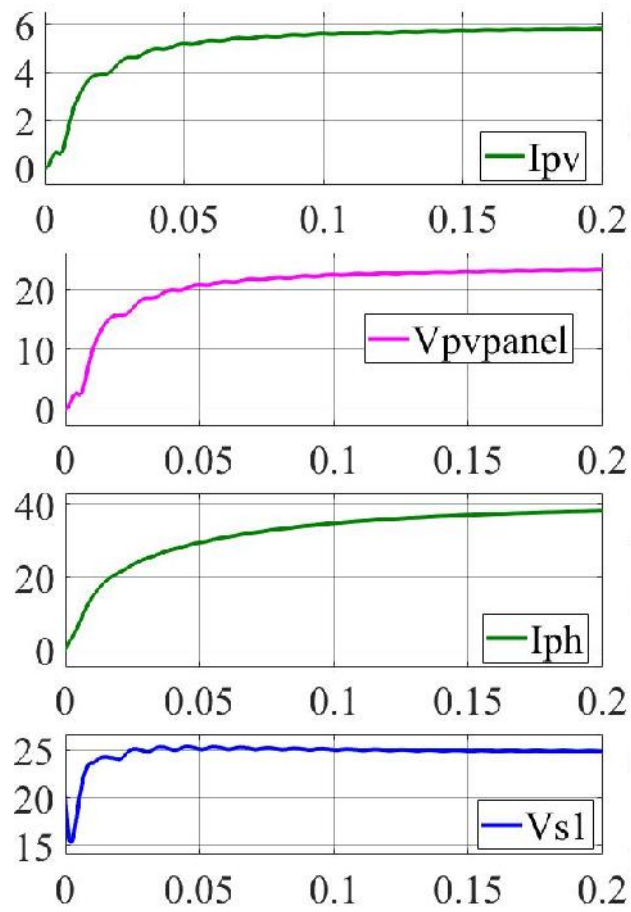
current i_{req} . This ensures storage current is regulated at a reference value selected based on the RSS. The reference storage current is selected as zero when source power is greater than load power, and SoC is greater than SoC_{max}. When SoC is less than SoC_{min} and source power is less than load power, the reference storage current is selected as $-i_{b,max}$. Therefore whenever grid current is zero, the excess or deficit power is taken care of by energy storage if not then by the grid. The switching pulses for the transformer-coupled half-bridge boost converter are generated based on the duty cycle selected by the selector switches S_2, S_3 . When the wind is OFF, the duty cycle is selected to be 0.5. When the wind is ON, the duty cycle generated by the PI controller is selected such that wind is operated at MPP by regulating i_w at i_{wmpp} . An inner current and outer voltage dual-loop control structure is used for a PHC. The reference voltage v_{pv} is selected as v_{mpp} when PV is available and is selected as $v_{dc1} - v_s$ when PV is OFF. PI voltage controller generates the required current i_{phr} to regulate v_{pv} at v_{pv} . The current controller generates the switching pulses for S_1 and S_2 such that i_{ph} is regulated at i_{phr} .

TABLE I. SYSTEM PARAMETERS

Parameters	Values
PV Source Parameters	
MPP Voltage (v_{pvmp})	20V
MPP Current (i_{pvmp})	4A
Energy Storage Unit:	
Nominal battery voltage (v_b)	24V
Rated battery capacity	32Ah
Internal battery resistance (r_b)	0.2Ω
Rated super capacitor voltage (v_{sc})	32V
Capacitance of Super capacitor (C_{sc})	9.6 F
Internal super capacitor resistance (r_{sc})	20 mΩ
Transformer turns ratio (n)	1 : 2
wind Parameters	
MPP voltage (v_{wmp})	20V
MPP Current (i_{wmp})	4A
Converter Parameters	
	$L_b=2$ mH, $L_{ph}=3$ mH, $L_w = 2$ mH, $C_{pv}= 2200$ μF $C_1=1000\mu F, C_2=1000\mu F$ $C_3=2$ $200\mu F, C_4=2200\mu F$
Grid Side Converter	$L_g = 10$ mH; $V_g = 40$ V
Load Parameters	10 - 100 Ω

IV. SIMULATION RESULTS AND DISCUSSIONS

MATLAB/Simulink is the platform used to simulate and validate the proposed system. The system is tested under all operating modes of RSS along with the basic functionality of ESU, i.e., diverting the high-frequency component power to supercapacitor during wind, PV, and load disturbances. The performance of the system during source and load changes when SoC > 80% and load power (PL) required is less than the source power (Ps) is shown in Fig. 8. The simulation results in Fig. 4 is depicting the PV panel output voltage and current.



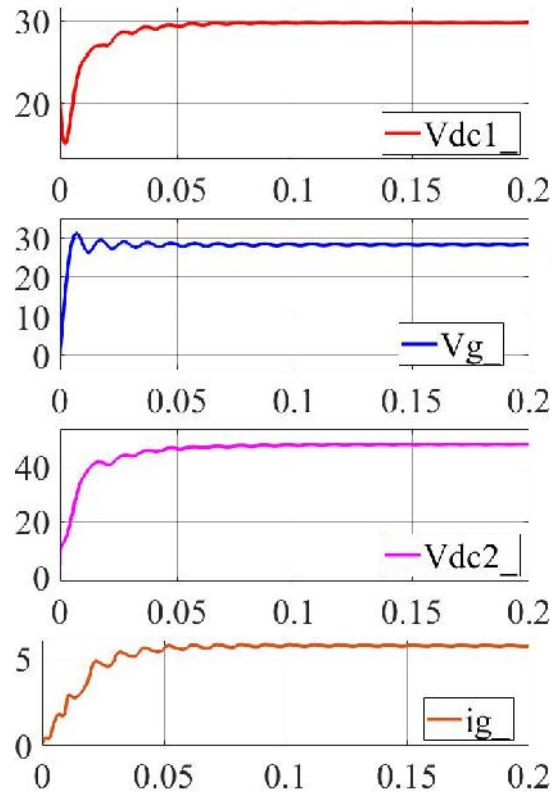


Fig. 4. PV panel voltage ($V_{pvpanel}$) and current (I_{pv}), phase current (I_{ph}), Supply Voltage (V_{s1}), The voltage across PHC (V_{dc1}), The grid side voltage (V_g), The voltage across CHBBC (V_{dc2}), Grid side current (i_g)

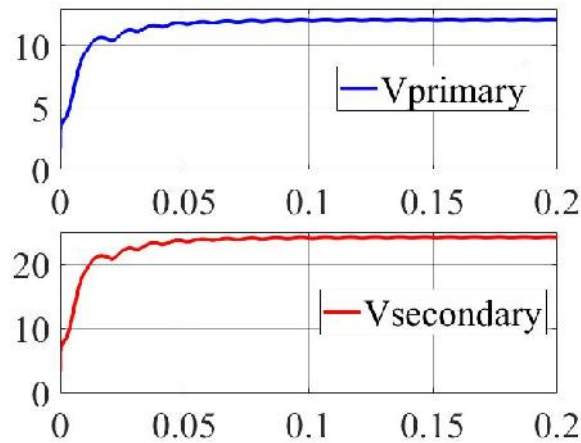


Fig. 5. Voltage across primary and secondary side of transformer ($V_{primary}$, $V_{secondary}$)

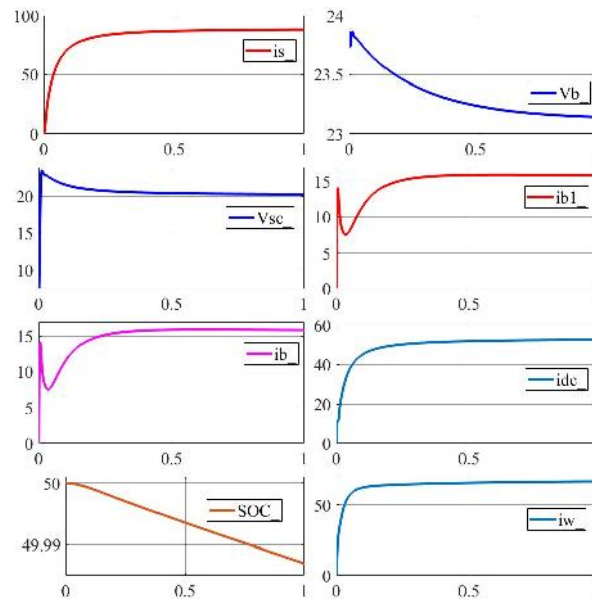


Fig. 6. Supply current (i_s), Voltage across super capacitor (V_{sc}), battery current (i_b), State of Charge (SOC), battery voltage (V_b), battery current (i_{b1}), current in PHC (i_{dc}), current in wind (i_w)

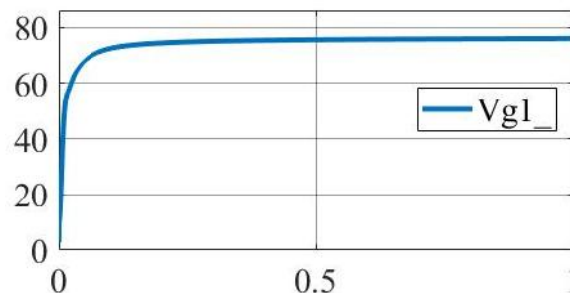


Fig. 7. Generated voltage (V_g)

The Renewable power generated is more than the required load power, and the battery is fully charged. Hence, the excess power generated is fed to the grid to maintain the power balance in the system.

V. CONCLUSION

The proposed isolated grid-connected multi-source converter configuration and control structure for the synergy of PV, wind, battery, and supercapacitor was developed and tested under respective operating modes. Energy storage supplies the power only if the SoC of battery is greater than 20%, else grid supplies. Energy storage takes power only if SoC of battery is less than 80%, else the grid takes the excess power. Also, the proposed system obeys the desired rules of renewable sources and ESU such as (iii) Operating at maximum power point and (iv) Diverting the transient peak current to the supercapacitor. The system gives a satisfactory performance during PV, wind, and load changes. The main advantages of the proposed system are the integration of ESU and renewable sources with less complexity in the control stage, less number of components, and galvanic isolation. Optimal tuning of controller parameters, designing a robust, fault-tolerant controller for the proposed converter configuration, will be considered as future work.

REFERENCES

- [1] A. M. Haddadi, S. Farhangi, and F. Blaabjerg, "A reliable three-phase single-stage multiport inverter for grid-connected photovoltaic applications," *IEEE J. Emerg. Sel. Topics Power Electron.*, vol. 7, no. 4, pp. 2384–2393, Dec. 2019.
- [2] Z. Tang, Y. Yang, and F. Blaabjerg, "An interlinking converter for renewable energy integration into hybrid grids," *IEEE Trans. Power Electron.*, vol. 36, no. 3, pp. 2499–2504, Mar. 2021.
- [3] A. U. Barbosa, B. R. de Almeida, D. d. S. Oliveira, P. P. Praça, and L. H. S. C. Barreto, "Multi-port bidirectional three-phase AC-DC converter with high frequency isolation," in *Proc. IEEE Appl. Power Electron. Conf. Expo.*, San Antonio, TX, USA, 2018, pp. 1386–1391.
- [4] H. S. Krishnamoorthy, D. Rana, P. Garg, P. N. Enjeti, and I. J. Pitel, "Wind turbine generator–battery energy storage utility interface converter topology with medium-frequency transformer link," *IEEE Trans. Power Electron.*, vol. 29, no. 8, pp. 4146–4155, Aug. 2014.
- [5] B. Mangu, S. Akshatha, D. Suryanarayana, and B. G. Fernandes, "Grid-connected PV-wind-battery-based multi-input transformer-coupled bidirectional DC-DC converter for household applications," *IEEE J. Emerg. Sel. Topics Power Electron.*, vol. 4, no. 3, pp. 1086–1095, Sep. 2016.
- [6] S. Neira, J. Pereda, and F. Rojas, "Three-port full-bridge bidirectional converter for hybrid DC/DC/AC systems," *IEEE Trans. Power Electron.*, vol. 35, no. 12, pp. 13077–13084, Dec. 2020.
- [7] D. Ma, W. Chen, L. Shu, X. Qu, and K. Hou, "A MMC-based multiport power electronic transformer with shared medium-frequency transformer," *IEEE Trans. Circuits Syst. II: Exp. Briefs*, vol. 68, no. 2, pp. 727–731, Feb. 2021.
- [8] O. Ray and S. Mishra, "Boost-derived hybrid converter with simultaneous DC and AC outputs," *IEEE Trans. Ind. Appl.*, vol. 50, no. 2, pp. 1082–1093, Mar./Apr. 2014.
- [9] J. Khodabakhsh and G. Moschopoulos, "Simplified hybrid AC–DC microgrid with a novel interlinking converter," *IEEE Trans. Ind. Appl.*, vol. 56, no. 5, pp. 5023–5034, Sep./Oct. 2020.
- [10] M. Rouhani and G. J. Kish, "Multiport DC–DC–AC modular multilevel converters for hybrid AC/DC power systems," *IEEE Trans. Power Del.*, vol. 35, no. 1, pp. 408–419, Feb. 2020.
- [11] Y. Li, D. Liu, and G. J. Kish, "Generalized DC-DC-AC MMC structure for MVDC and HVDC applications," in *Proc. 20th Workshop Control Model. Power Electron.*, Toronto, ON, Canada, 2019, pp. 1–8.
- [12] M. Vasiladiotis and A. Rufer, "A modular multiport power electronic transformer with integrated split battery energy storage for versatile ultrafast EV charging stations," *IEEE Trans. Ind. Electron.*, vol. 62, no. 5, pp. 3213–3222, May 2015.
- [13] G. Waltrich, J. L. Duarte, and M. A. M. Hendrix, "Multiport converter for fast charging of electrical vehicle battery," *IEEE Trans. Ind. Appl.*, vol. 48, no. 6, pp. 2129–2139, Nov./Dec. 2012.
- [14] J. Kan, S. Xie, Y. Wu, Y. Tang, Z. Yao, and R. Chen, "Single-stage and boost-voltage grid-connected inverter for fuel-cell generation system," *IEEE Trans. Ind. Electron.*, vol. 62, no. 9, pp. 5480–5490, Sep. 2015.
- [15] Q. Sun, J. Wu, C. Gan, J. Si, J. Guo, and Y. Hu, "Cascaded multiport converter for SRM-based hybrid electrical vehicle applications," *IEEE Trans. Power Electron.*, vol. 34, no. 12, pp. 11940–11951, Dec. 2019.
- [16] J. He, L. Du, S. Yuan, C. Zhang, and C. Wang, "Supply voltage and grid current harmonics compensation using multiport interfacing converter integrated into two-AC-bus grid," *IEEE Trans. Smart Grid*, vol. 10, no. 3, pp. 3057–3070, May 2019.
- [17] W. Cai, L. Jiang, B. Liu, S. Duan, and C. Zou, "A power decoupling method based on four-switch three-port DC/DC/AC converter in DC microgrid," *IEEE Trans. Ind. Appl.*, vol. 51, no. 1, pp. 336–343, Jan./Feb. 2015.
- [18] H. Wu, L. Zhu, and F. Yang, "Three-port-converter-based single-phase bidirectional AC–DC converter with reduced power processing stages and improved overall efficiency," *IEEE Trans. Power Electron.*, vol. 33, no. 12, pp. 10021–10026, Dec. 2018.



Volume 6- Issue 1, Paper 5, January 2023

- [19] N. Kim and B. Parkhideh, "PV-battery series inverter architecture: A solar inverter for seamless battery integration with partial-power DC–DC optimizer," *IEEE Trans. Energy Convers.*, vol. 34, no. 1, pp. 478–485, Mar. 2019.
- [20] K. Wang, R. Zhu, C. Wei, F. Liu, X. Wu, and M. Liserre, "Cascaded multilevel converter topology for large-scale photovoltaic system with balanced operation," *IEEE Trans. Ind. Electron.*, vol. 66, no. 10, pp. 7694–7705, Oct. 2019.
- [21] H. Moradisizkoochi, N. Elsayad, M. Shojaie, and O. A. Mohammed, "PWM plus phase-shift-modulated three-port three-level soft switching converter using GaN switches for photovoltaic applications," *IEEE J. Emerg. Sel. Topics Power Electron.*, vol. 7, no. 2, pp. 636–652, Jun. 2019.
- [22] J. Deng, H. Wang, and M. Shang, "A ZVS three-port DC/DC converter for high-voltage bus-based photovoltaic systems," *IEEE Trans. Power Electron.*, vol. 34, no. 11, pp. 10688–10699, Nov. 2019.
- [23] S. Hu, Z. Liang, and X. He, "Ultracapacitor-battery hybrid energy storage system based on the asymmetric bidirectional z-source topology for eV," *IEEE Trans. Power Electron.*, vol. 31, no. 11, pp. 7489–7498, Nov. 2016.